OPEN

Immediate Enhancement of Nerve Function Using a Novel Axonal Fusion Device After Neurotmesis

David Colton Riley, BS, Richard B. Boyer, MD, PhD,* Curt A. Deister, PhD,† Alonda C. Pollins, MS,* Nancy L. Cardwell, BS, Nathaniel D. Kelm, BS,‡ Mark D. Does, PhD,‡ Richard D. Dortch, PhD,§ Ravinder Bamba, MD,* Robert Bruce Shack, MD,* and Wesley P. Thayer, MD, PhD**

Background: The management of peripheral nerve injuries remains a large challenge for plastic surgeons. With the inability to fuse axonal endings, results after microsurgical nerve repair have been inconsistent. Our current nerve repair strategies rely upon the slow and lengthy process of axonal regeneration (~1 mm/d). Polyethylene glycol (PEG) has been investigated as a potential axonal fusion agent; however, the percentage of axonal fusion has been inconsistent. The purpose of this study was to identify a PEG delivery device to standardize outcomes after attempted axonal fusion with PEG.

Materials and Methods: We used a rat sciatic nerve injury model in which we completely transected and repaired the left sciatic nerve to evaluate the efficacy of PEG fusion over a span of 12 weeks. In addition, we evaluated the effectiveness of a delivery device's ability to optimize results after PEG fusion.

Results: We found that PEG rapidly (within minutes) restores axonal continuity as assessed by electrophysiology, fluorescent retrograde tracer, and diffusion tensor imaging. Immunohistochemical analysis shows that motor axon counts are significantly increased at 1 week, 4 weeks, and 12 weeks postoperatively in PEG-treated animals. Furthermore, PEG restored behavioral functions up to 50% compared with animals that received the criterion standard epineurial repair (control animals).

Conclusions: The ability of PEG to rapidly restore nerve function after neurotmesis could have vast implications on the clinical management of traumatic injuries to peripheral nerves.

Key Words: peripheral nerve injury, neurotmesis, nerve transection, Wallerian degeneration, traumatic neuropathy, axonal fusion, polyethylene glycol, diffusion tensor tractography

(*Ann Plast Surg* 2017;79: 590–599)

Peripheral nerve injuries can result in life-long pain and disability. Extremity trauma is responsible for most Americans who suffer from peripheral nerve injury.[1,2] These injuries disproportionately affect the younger and healthy civilian population, as well as military members, who are at greater risk for traumatic injuries.[2] Advances in the treatment of military and civilian injuries have increased the number of survivors from motor vehicle accidents and military trauma, which have further increased the number of patients living with mutilated extremities. In fact, for some traumatic extremity injuries, the expected poor recovery of nerve function is an indication for completion amputation over replantation. Despite improvements in the understanding of peripheral nerve injury pathophysiology, epineurial repair remains the criterion standard for surgical nerve reconstruction with a continued reliance on the slow and inefficient process of peripheral nerve growth.[3]

Factors such as a patient's age, type of injury, location of injury, and delay before intervention play a critical role in determining the potential recovery after traumatic injury to peripheral nerves.[3] The poor clinical outcomes of peripheral nerve injury are due in large part to the slow and lengthy process of axonal elongation. In order for practical recovery to occur, axons in the proximal stump must reach their target muscles and remake functional connections. Muscle atrophy initiates immediately after muscle denervation and plateaus after approximately 3 to 4 months after 60% to 80% loss in muscle volume.[4] In addition, motor axons must reach the target muscle in a critical time window (12–18 months). After this time period, muscle is less amenable to reinnervation.[5] In the case of neurotmesis (Sunderland Type V), it is estimated that there is a 50% loss of axons across each coaptation site. Furthermore, of the small percentage of axons that do reach their target muscle, it is estimated that even a smaller percentage are able to remake functional connections.[6] Axonal regeneration occurs over lengths of up to 1 m in humans, making recovery lengthy and minimally effective. For example, complete brachial plexus injuries have anticipated recovery times ranging from 2 to 3 years after repair, with such cases being recognized clinically as having little to no chance of restored motor or sensory function in the distal-most targets of the hand. In most cases, surgeons agree on elbow flexion as the ultimate measure of surgical success in the event of complete brachial plexus severance.[7,8]

Received November 20, 2016, and accepted for publication, after revision August 8, 2017.

From the *Department of Plastic Surgery, Vanderbilt University Medical Center, Nashville, TN; †Axogen Corporation, Alachua, FL; ‡Vanderbilt University Institute of Imaging Science; and §Department of Radiology and Radiological Sciences, Vanderbilt University, Nashville, TN.

Conflicts of interest and sources of funding: This work was supported by the Department of Defense: Grant Number OR120216–Development of Class II Medical Device for Clinical Translation of a Novel PEG Fusion Method for Immediate Physiological Recovery after Peripheral Nerve Injury. C. Deister is a Product Development Engineer at Axogen Inc, which is a company that produces nerve repair devices. Axogen was listed as a co-investigator on the DOD grant. Axogen was not involved in the financial funding in this study. The other authors have no conflicts of interest to declare.

Portions of this work were presented in abstract form at the American Association of Neurological Surgeons Annual Meeting in May 2015 and the Plastic Surgery Research Council Annual Meeting in May 2015.

D.C. Riley contributed in the study design, surgery, data acquisition, data analysis, and writing. R.B. Boyer also worked on the study design, data acquisition, and data analysis. C.A. Deister worked on the study design, data analysis, and writing. A. C. Pollins also contributed in the study design, data acquisition, data analysis, and writing. N.L. Cardwell was also responsible for the study design, data acquisition, data analysis, and writing. N.D. Kelm worked on the data acquisition, data analysis, and writing. M.D. Does also contributed in the data acquisition, data analysis, and writing. R. D. Dortch worked on the data acquisition, data analysis, and writing. R. Bamba was also responsible for the study design, data analysis, writing, and critical revision. R.B. Shack also worked on the study design, data analysis, writing, and critical revision. W.P. Thayer was also responsible for the study design, data analysis, writing, and critical revision.

Reprints: David Colton Riley, BS, Vanderbilt University Medical Center North, 1161 21st Ave S, S-2221, Nashville, TN 37232. E-mail: dcolton.riley@gmail.com.

ISSN: 0148-7043/17/7906–0590
DOI: 10.1097/SAP.0000000000001242

Current research strategies are focused on enhancement of axonal regeneration and/or a reduction in environmental inflammation given the lack of ability to fuse severed axonal endings. Biological roadblocks such as Wallerian degeneration have hampered clinicians and neuroscientists from developing a rapid and effective technique to significantly augment recovery after traumatic injuries to peripheral nerves.[9,10] However, it has been observed in many phyla that severed peripheral nerves naturally, rapidly, and effectively restore lost nerve function via outgrowths from proximal stumps that fuse and/or activate functional connections.[10,11] For decades, scientists have used the hydrophilic properties of polyethylene glycol (PEG) to fuse together cells to immortalize desired cell lines such as monoclonal antibody producing B cells.[12] Taking advantage of the hydrophilic properties of PEG, medial giant axons of giant squid were first fused in 1986.[13] Closely apposed ends of severed earthworm medial giant axons have since been artificially fused by PEG,[14,15] laser beams,[16] and electric fields.[17] Building on these reports, researchers demonstrated that both physiologic and behavioral recovery could be regained in a crushed rat sciatic nerve model.[18] We recently reported the first successful fusion of severed mammalian nerves that demonstrated long-term histological and behavioral improvements.[19]

Although the mechanism of PEG fusion is unknown, it is hypothesized that PEG enables lipid bilayer fusion by removing H_2O molecules surrounding the axolemma and allowing the lipid membranes to flow together.[20] In our modified PEG fusion technique, we use a sequence of steps to rapidly re-establish axonal continuity and restore up to 50% lost behavioral function in a rat sciatic nerve injury model. Our protocol involves irrigating the injured nerve in an isotonic, calcium-free solution to maintain open axonal ends. In addition, methylene blue (MB), an antioxidant, is added to the nerve ends to prevent/reduce vesicle formation. Once the nerve ends have been reapproximated, typically through the use of microsutures, PEG is added to induce membrane fusion between open axonal ends. Polyethylene glycol is then washed away by an isotonic, calcium containing solution to seal the remaining holes in the axolemma (Fig. 1).

Previous in vivo and ex vivo studies have shown inconsistencies in morphological and functional recovery of PEG-fused animals.[19,21,22] The data suggest that factors such as the quality of repair, time of surgical intervention, and a surgeon's level of experience with the technique play a critical role in achieving successful PEG fusion.[19,21–23] A deficiency of surgeons with subspecialty training in peripheral nerve injury has emphasized the need for a device to simplify and

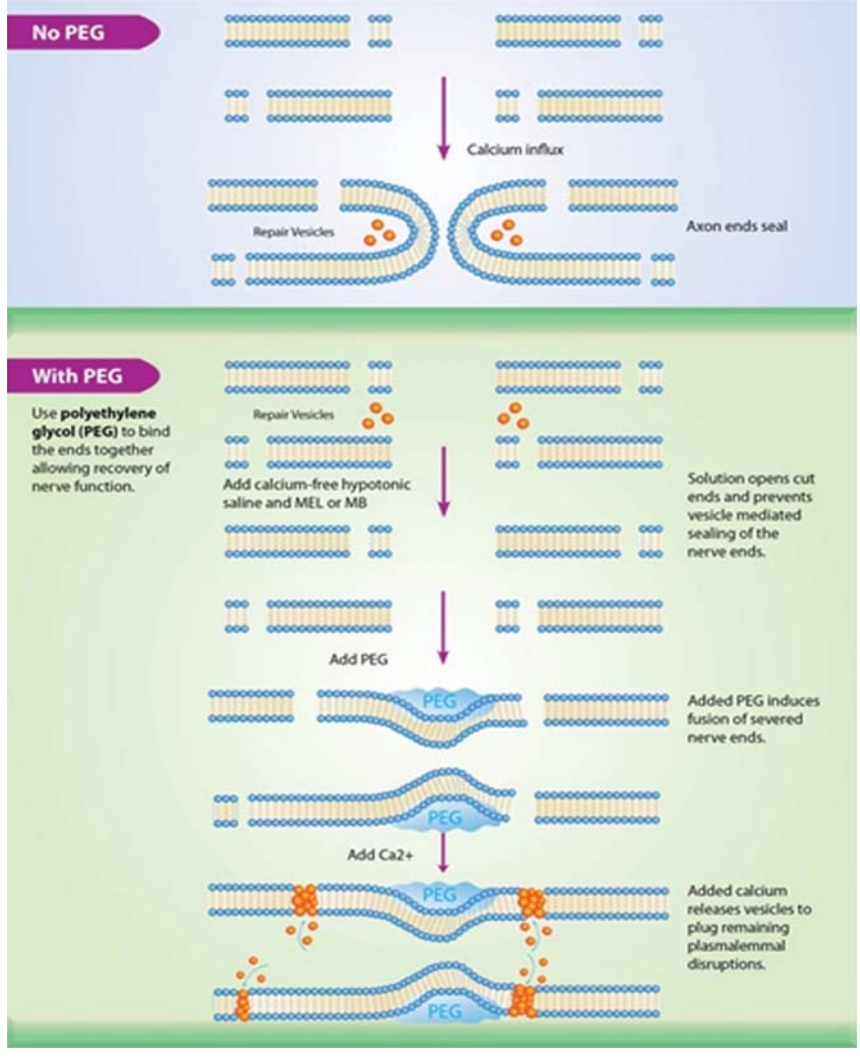

FIGURE 1. Mechanism of PEG axonal fusion. In the absence of PEG, calcium-mediated vesicles form and seal axonal endings, preventing fusion. The PEG and MB or melatonin reduce vesicle formations and promote axonal fusion. Reprint from Rodriquez-Feo (2013).

improve functional results of peripheral nerve repairs in the clinic.[24,25] Previous studies have applied the PEG solution manually through a syringe with the needle held at the surface of the neurorrhaphy. Manual application of PEG is subject to inconsistency in PEG delivery to the neurorrhaphy site. A simple delivery device, which secures a short needle at the anastomosis and can be removed without disturbing the neurorrhaphy, could remove some of the sources of manual variability from PEG-based nerve fusion.

MATERIALS AND METHODS

All experimental procedures were approved by and performed in accordance with the standards set forth by the Institutional Animal Care and Use Committee at Vanderbilt University. Every effort was made to minimize the amount of suffering of animals in the study. Animals were caged in groups of 3 and supplied with water and food (Purina Rodent Diet) at all times. Animal cages were inspected daily to ensure animal health and cleanliness of housing by both the Vanderbilt Veterinary staff and surgical research personnel.

Experimental Design

The objective of this study was to evaluate the efficacy of PEG-fusion nerve repair and optimize a device for effective delivery of PEG into the neurorrhaphy. We used a rat sciatic nerve injury model to evaluate the following 3 groups: cut + repair (control, n = 30), cut + repair + PEG (PEG, n = 30), and cut + repair + PEG (device) (PEG [device], n = 30). The entire study required a total of 96 animals (an additional group of rats [n = 6] were used as unoperated control for retrograde analysis).

PEG Delivery Device

The devices were assembled under 4× loupe magnification. First, a 4- to 5-mm length (blunt ended) 27G stainless steel tubing cut from a hypodermic needle was inserted inside a 5.5-cm length of 3-French silicone tubing (Strategic Applications, Inc) using high viscosity epoxy adhesive (Loctite Ultra Gel Control Super Glue). Approximately 0.5 to 1 mm of blunt needle was present outside of the silicone tubing. The hub of the 27-G hypodermic needle was then trimmed to approximately 15 mm in tubing length and attached to the other end of the silicone tubing. This construct was then cured overnight and checked for patency and fluid flow. A 1 × 15-cm strip of 3 mil polyethylene sheeting was attached to the silicone tubing by coating the sheeting with a film of silicone adhesive and aligning the entubulated end of the blunt needle stub at the start of the silicone adhesive before pressing the tubing into the film and allowing to cure overnight. Five punctures in the sheeting were made with a 27-G needle before silicone adhesive application to allow the adhesive to set within the punctures and increase the retention strength.(Figs. 2, 3)

Surgical Procedures

Female Sprague-Dawley rats (n = 96) were anesthetized via inhaled isoflurane (2%). A 3-cm dermal incision was made parallel and just posterior to the left femur. Using sharp dissection, the cephalad border of the biceps femoris was manipulated to allow for exposure of the left sciatic nerve. Once exposed, the nerve was trimmed free of any perineural connective tissue. The exposed nerve was thoroughly rinsed in a calcium-free saline, Plasmalyte-A (Baxter, Deerfield, Ill). Electrophysiological testing was performed to obtain baseline preinjury compound action potential (CAP) conduction recordings.

A complete transection of the left sciatic nerve was made to imitate a Sunderland-type V nerve injury. The wound was bathed in additional Plasmalyte-A, and the nerve ends resected back even with the epineurium. Immediately after, a 1% MB solution was applied to both nerve ends. Using standard microsurgical technique, a standard end-to-end nerve repair was made using 9-0 ethilon (Ethicon, Somerville, NJ) under a surgical microscope. The PEG and PEG (device) animals had 1 mL of PEG through either a standard hand-held needle (PEG group) or a nerve wrap with the delivery device described previously (PEG [device] group) for 1 minute. All experimental animals received PEG within 2 hours after injury. Control animals did not receive PEG.

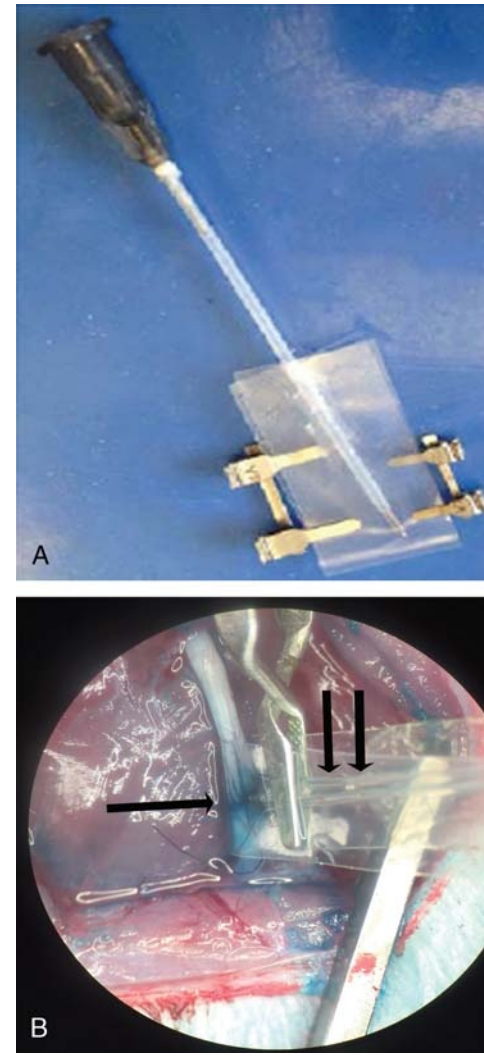

FIGURE 2. A, Nerve wrap with needle secured by clips. B, Nerve wrap implanted on a rat sciatic nerve. The single arrow indicates the nerve repair site inside the nerve wrap. The double arrow indicates the needle inside the nerve wrap through which PEG is delivered.

The wound was flushed with a calcium-containing saline, lactated ringer's (Hospira, Lake Forect, Ill), until all residual PEG was rinsed free from the injury site. Postrepair CAPs were tested for CAPs across the injury site. The skin was reapproximated using a running subcuticular 5-0 monocryl suture (Ethicon). All survival animals received a subcutaneous injection of ketoprofen (5 mg/kg) and were allowed to recover from anesthesia under careful monitoring. In addition, injections of ketoprofen were made daily for 3 days postoperation.

No animals died during surgical procedures or were euthanized before planned endpoints. In the case of illness or injury, as assessed by Vanderbilt University Animal Care Veterinary staff, animals would be euthanized within 24 hours of discovery via intracardiac injection of euthasol. The dysesthesia and paresthesia that occurs in laboratory

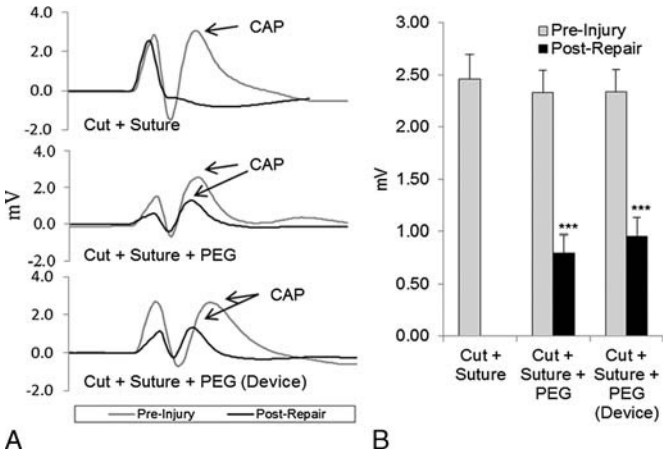

FIGURE 3. A, Representative CAPs recorded preinjury (gray traces) and postrepair (dark traces) from a control, PEG-fused, and PEG-fused [device] nerve. B, The CAPs (mV, mean ± SE) recorded preinjury and postrepair for 3 groups: cut + suture (n = 18), cut + suture + PEG (n = 18) cut + suture + PEG (device) (n = 18). The PEG treatment groups demonstrated statistically significant ($P < 0.001$: ***) physiological recovery compared with the cut + suture group.

rats after peripheral nerve injury results in autophagy and self-mutilation of the affected limb. Symptoms such as "toe-biting" can be seen as early as 2 to 3 weeks postinjury. This destructive behavior interferes with functional assessments such as the footfault asymmetry and sciatic functional index tests. To prevent as much autophagy and self-mutilation as possible, the rats were monitored daily for all preliminary signs. Rats that showed signs of autophagy had the affected limb coated with a bitter topical mixture (Thum; Oakhurst Company Levittown, NY) that has been shown to minimize autophagy. All animals were euthanized via intracardiac injection of euthasol (euthanasia solution).

Electrophysiological Testing

Compound action potentials are a measure of axonal continuity and conduction between electrodes.[14,19] All CAPs (n = 54;) were obtained with a PowerLab data acquisition system (AD Instruments, Colorado Springs, Colo) interfaced with a LabChart 7 (Ad Instruments). A stimulating electrode was placed under the sciatic nerve proximal to the injury, whereas the recording electrode was placed under the sciatic nerve distal to the repair site. The CAPS were recorded at 2 separate time points: before the injury (preinjury) and immediately after application of Ca^{2+} containing saline rinse (postrepair).

Retrograde Tracer

We performed analysis of axonal continuity using a retrograde tracer technique on a subset of rats in each group (unoperated control, n = 6; control, n = 6; PEG, n = 6; PEG [device], n = 6). Immediately after repair, the nerve was transected distal to the repair, and the proximal end was dipped into a polypropylene tube containing 5 μL of 2% fast blue retrograde tracer (Polysciences, Inc, Warrington, Pa). After 1 hour, the excess tracer has washed off the nerve with calcium-free solution (Plasmalyte A). The skin was reapproximated using a running subcuticular 5-0 monocryl suture (Ethicon). One week later, the rats were anesthesized with 3% isoflurane and then injected with a mixture of Ketamine (100 mg/kg) + xylazine (10 mg/kg) intraperitoneally in the right lower quadrant. After 5 minutes of induction time, the animals are perfusion fixed, intracardially, with 150 mL of 1X phosphate buffered saline (PBS) and 250 mL of 4% paraformaldehyde. The left sciatic nerve and the spinal cord from L2 to L4 segments were dissected. The sciatic nerve and spinal cord segment was washed twice in 1X PBS after isolation from the animal. The tissue is immediately frozen with OCT using dry ice. Sciatic nerve and spinal cord cross sections are made at 30 microns with cryostat and serially mounted on glass slides. The sections are immediately examined under the Nikon AZ100M wide field fluorescent microscope using the DAPI filter to examine fast blue fluorescent tracer (excitation, 365 nm; emission, 420 nm). The neuronal cells with identifiable nucleus were counted in every 10th section of the spinal cord. Fast blue labels the cytoplasm producing intense blue fluorescence with a central dark nucleus. Some cells also had nuclear staining with white to bluish fluorescence.

Behavioral Testing

Behavioral assessments were performed at 3 days followed by weekly intervals up to 12 weeks, postoperatively. Animals were not tested earlier to allow adequate time to recover from the effects of ketoprofen administration at the time of surgery. People blind to the treatment assessed behavioral measurements in an effort to eliminate possible bias. Each animal underwent the foot fault (FF) asymmetry and sciatic functional index test at each time point. In addition, each animal that was behaviorally assessed underwent electrophysiology testing (CAP recordings) at the time of surgery.

FF Asymmetry Score

Animals were allowed to roam freely on a wire mesh grid measuring 45 × 30 cm, with square openings measuring 2.5 × 2.5 cm. The grid was elevated 2 cm above a solid base. Trials of 50 total steps for each hind limb were recorded for each animal individually. A full fault was recorded if the animal's hind limb fell through the opening in the grid and touched the floor. A partial fault was recorded in the event that the animal's hind limb fell through the opening but did not touch the floor. We calculated a composite FF score using the previously reported and following equation[19,26]: composite FF score = (n partial faults × 1) + (n full faults × 2), %FF = (composite FF score/total number of steps) × 100%, FF asymmetry score = %FF (normal hind limb) − %FF (surgical hind limb).

Sciatic Functional Index

The Sciatic Functional Index (SFI) is a well-established measure of sciatic function that includes both sensory feedback and motor control.[19,26,27] Before surgery, rats were trained to transverse an inclined beam into a home cage. After these initial habituation trials, the rats would navigate the beam into their cage without hesitation. The hind limbs were inked, such that black designated the unoperated limb and red designated the surgical limb. Animals were placed on the beam farthest from the cage, and 6 consecutive (3 from each limb) foot prints were recorded. As previously published, the SFI was scored in the following manner. Normal print length (NPL), normal toe spread (NTS), normal intermediary toe spread (NIT), Experimental print length (EPL), experimental toe spread (ETS), and experimental NIT. Print length is measured from the heel to the tip of toe 3, toe spread was measured from toes 1 to 5, and NIT was measured from toes 2 to 4. The SFI scores were calculated using the following formula: SFI = −38.3([EPL − NPL]/NPL) + 109.5([ETS − NTS]/NTS) + 13.3([EIT − NIT]/NIT) − 8.8. An SFI score of −100 or less indicates complete loss of sciatic nerve function, and scores of −10 or greater indicate normal sciatic nerve function.

Histology

We performed analysis of axonal counts using an immunohistochemistry staining technique on a subset of rats (n = 54) in each group (control, PEG, and PEG [device]) at 3 separate time points [1 week

(n = 6/group), 4 weeks (n = 6/group), and 12 weeks (n = 6/group)]. Immunohistochemical staining was performed using commercial antibodies specifically directed against choline acetyltransferase (Millipore, Temecula, Calif). Formalin-fixed, paraffin-embedded tissues were sectioned at 5 mm, placed on slides, and warmed overnight at 60°C. Slides were deparaffinized and rehydrated with graded alcohols ending in Tris-buffered saline (TBS-T Wash Buffer; LabVision, Freemont, Calif). Heat-mediated target retrieval was performed in 1X Target Retrieval Buffer (DAKO, Carpinteria, Calif) using a Decloaking chamber (BioCare Medical, Concord, Calif) with the following settings: SP1 at 125°C for 1 minute and SP2 at 90°C for 10 seconds. Slides were then removed from the chamber and allowed to cool on the bench for 20 minutes, after which they were placed in TBS-T for at least 3 minutes before proceeding. Endogenous peroxidases were blocked by incubation in 3% H2O2 (Fisher, Suwanee, Ga) in TBS-T for 40 minutes. Nonspecific background (40 minutes), secondary (30 minutes), and tertiary labeling (30 minutes) of target was accomplished by use of Vector ABC Elite Goat IgG kit (Vector Laboratories, Burlingame, Calif). Primary antibody to choline acetyltransferase was used at 1:200 for 1 hour. Slides were rinsed with TBS-T between each reagent treatment, and all steps were carried out at room temperature. Visualization was achieved with DAB+ chromogen (DAKO). Slides were counterstained with Mayer's hematoxylin, dehydrated through a series of alcohols and xylenes, and then coverslipped with Acrytol Mounting Media (Surgipath, Richmond, Ill).

Diffusion Tensor Magnetic Resonance Imaging

We performed diffusion tensor magnetic resonance imaging (MRI) on each group. Nerves were harvested immediately after repair for imaging.

Tissue Sample Preparation

After 24 hours of postfixation, excised nerves were placed in PBS + 2 mM Gd-DTPA (Magnevist; Bayer HealthCare, Wayne, NJ) at 4°C for at least 24 hours before imaging. For imaging, excised nerves were trimmed to 1 cm in length (with the injury site centered) and placed in a 2-mm outer diameter glass capillary tubes filled with a perfluoropolyether liquid (Fomblin; Solvay Solexis, Thorofare, NJ) for susceptibility matching, preventing tissue dehydration, and a signal-free background. For higher throughput, 6 excised sciatic nerves in a hexagonal arrangement were imaged simultaneously. Hind limb samples were postfixed for a period of 1 week, followed by at least 1 week of washing in PBS + 2 mM Gd-DTPA before imaging. For imaging, hind limbs were placed in MR-compatible tubes filled with perfluoropolyether liquid.

Diffusion Tensor MRI

The MRI was performed on a 4.7-T 31-cm horizontal bore Agilent DirectDrive scanner (Agilent Technologies, Santa Clara, Calif) using a 38-mm Litz quadrature coil (Doty Scientific, Columbia, SC) for radiofrequency transmission and reception. For excised nerve imaging, field of view = 9.6 × 9.6 × 12 mm3 and matrix size = 96 × 96 × 32 for a nominal resolution of 100 × 100 × 375 mm3 (375 mm along the nerve). For hind limb imaging, field of view = 48.0 × 25.6 × 28.8 mm3 and matrix size = 192 × 128 × 144 for a nominal resolution of 250 × 200 × 200 mm3 (250 mm along the nerve). Diffusion tensor imaging (DTI) data were acquired using a 3D diffusion-weighted spin-echo sequence with TR/TE of 170/23.0 milliseconds and 12 signal averages for excised nerves, and TR/TE of 170/22.1 milliseconds and 2 signal averages for hind limbs. Diffusion weighting was achieved with δ/Δ = 4/12 milliseconds, prescribed b-value = 2000 seconds/mm2, and 6 directions. One b = 0 image was acquired for a total of 7 images in a scan time of 12 hours.

DTI Postprocessing and Analysis

Image data reconstruction was performed in MATLAB (Mathworks, Natick, Mass), and DTI analysis was implemented using ExploreDTI. During reconstruction from k-space data, 3D image volumes were zero-padded 2× in each direction. Then, a diffusion tensor for each voxel was estimated using a linear least-squares approach. From the diffusion tensor, DTI metrics including fractional anisotropy (FA) and mean, axial and radial diffusivity (mean diffusivity [MD], axial diffusivity, and radial diffusivity, respectively) were computed on a voxel-wise basis, and DTI tractography was performed.

Statistical Analyses

All statistical analyses were performed using GraphPad Prism (GraphPad Software, San Diego, Calif). To compare CAPs, MR DTI, and retrograde tracer analysis, we used a Kruskal-Wallis with Dunn's multiple comparison test. Behavioral tests (fault asymmetry [FF] and SFI scores) were compared using a two-way analysis of variance with the Bonferroni multiple comparison method. This allowed for specific comparisons between treatment and control groups. For motor axon counts, we used a Student *t* test to compare specific groups. All *P* values were two-tailed. All means were reported with their respective standard error values (mean ± SE).

RESULTS

Electrophysiology of Sciatic Nerves

The CAPs were evaluated at 2 time points: preinjury and postrepair (Fig. 3). The CAPs were recorded by stimulating the entire rat sciatic nerve. To prevent possible electrical stimulation across the injury site, the stimulating electrode was placed a minimum of 1 cm proximal to the injury and the recording electrode 0.5 cm distal. Electrophysiological studies showed that preinjury CAPs were present in all animals (n = 54). The CAPs were associated with a twitch in the muscles they innervated in the lower calf and foot. No statistically significant differences in CAP amplitudes were detected between control (mean: 2.46 ± 0.24 mV, n = 18), PEG (mean: 2.33 ± 0.21 mV, n = 18), and PEG [device] groups (mean: 2.34 ± 0.21 mV, n = 18) before complete transection of the rat sciatic nerve. After 100% transection and repair of the sciatic nerve, no CAPs were recorded in any control animals. By contrast, we found that 72% (13/18) of PEG and 83% (15/18) of PEG (device) animals had restored CAP function within minutes after repair and application of PEG (Fig. 3A). Postrepair CAP recordings for both PEG (mean: 0.80 ± 0.18 mV) and PEG (device) (mean: 0.96 ± 0.17 mV) groups were significantly decreased compared with their respective preinjury CAP amplitudes, however, both exhibited a statistically significant improvement in-post repair CAP amplitudes ($P < 0.001$ and $P < 0.001$, respectively) compared with controls (Fig. 3B). No statistical difference was found between PEG and PEG (device) postrepair CAP recordings.

Retrograde Labeling of Spinal Motor Neurons

Fast blue, a fluorescent retrograde label, was used to assess axonal continuity as well as intra-axonal transport across the injury site in uncut (n = 6), control (n = 6), PEG (n = 6), and PEG (device) (n = 6) nerves. Fluorescent spinal motor neurons labeled by fast-blue tracer were counted from L2 to L4 of rat spinal cords (Fig. 4). Morphological data showed that the fluorescent label was transported intracellularly in all uncut nerves (mean, 179.83 ± 14.74). However, only a minimal number of spinal motor neurons were labeled in control animals (mean, 2.33 ± 1.96). The PEG animals were associated with a statistically significant ($P < 0.05$) increase in the number of retrograde labeled cells (mean: 38.50 ± 9.45, n = 6). Using the delivery device, PEG (device) animals showed an even higher statistically significant increase

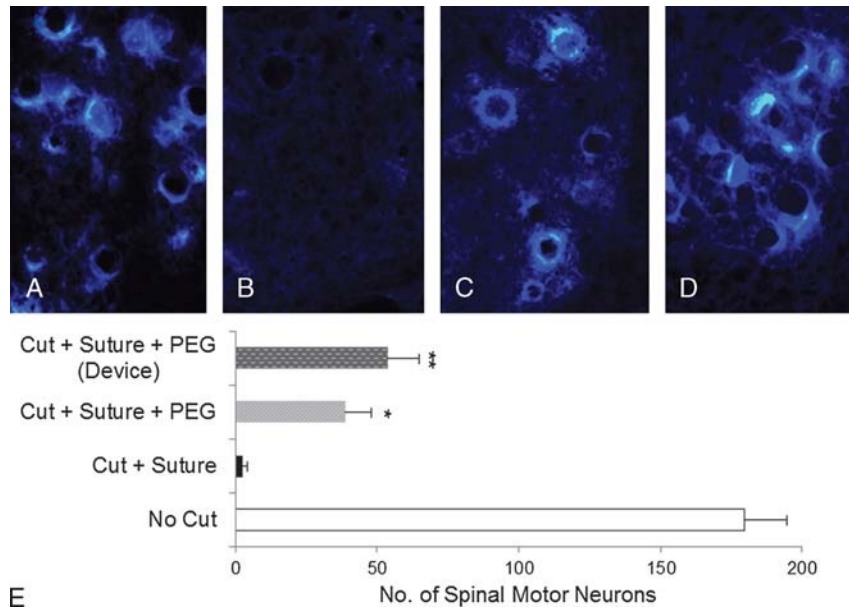

FIGURE 4. Fast blue retrograde labeling of sciatic spinal motor neurons. Representative cross sections taken from L2 to L4 of the spinal cord showing neuronal cells labeled with fast blue retrograde tracer from an (A) uncut control, (B) control, (C) PEG, and (D) PEG (device) animal. Fluorescent spinal motor neurons (mean ± SE) were counted from 150 cross sections (E). The PEG and PEG (device) groups (E) were associated with a statistically significant increase ($P < 0.05$ and $P < 0.01$, respectively) in the number of fast-blue labeled cells.

($P < 0.01$) in the number of labeled spinal motor neurons (mean: 53.50 ± 11.45, n = 6) compared with control animals. The number of labeled cells in both PEG and PEG (device) animals were significantly less ($P < 0.001$) compared with uninjured nerves.

DTI of Surgically Repaired Sciatic Nerves

The DTI of excised sciatic nerves (Fig. 5) were assessed at 3 regions of interest (ROI): repair site, 5 mm proximal, and 5 mm distal. A margin of approximately 100 μm around the exterior of the nerve was excluded to prevent partial volume effects and eliminate suture material in ROI calculations. The FA and MD were used to evaluate each ROI. The FA did not statistically differ in either the proximal or distal ROIs among control (n = 6), PEG (n = 6), and PEG (device) (n = 6) groups. All animals were associated with decreased FA at the site of injury compared with the proximal ROI. However, PEG and PEG (device) groups were associated with significantly higher FA at the repair site ($P < 0.05$ and $P < 0.01$, respectively) compared with controls. As expected,

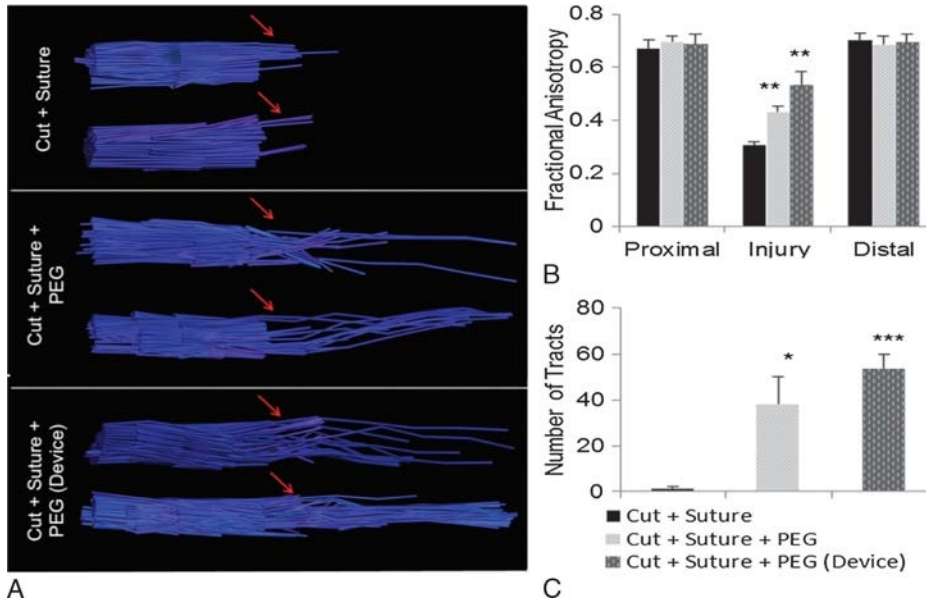

FIGURE 5. Diffusion tensor tractography of fixed rat sciatic nerves. A, Representative tractography of transected nerves harvested immediately after repair: control (left), PEG (middle), and PEG (device) (right). Green arrows indicate zone of repair. B, The FA and (C) number of tracts (mean ± SE) at the site of injury displayed significant increases in PEG and PEG (device) groups.

control animals were associated with the lowest value of MD and highest value of radial diffusivity of the 3 groups. Continuous fiber tracking was achieved by creating seed points at the 5 mm proximal ROI and tracing through the repair site until the 5 mm distal ROI (10 mm tract length). Representative tractography images (Fig. 5A) show that axonal tracts do not extend more than a couple millimeters distal to the repair site in control nerves. The PEG (mean: 38.17 ± 7.68, n = 6) and PEG (device) (mean: 53.83 ± 7.68, n = 6) groups both exhibited a statistically significant increase in the number of tracts that travelled through the repair site ($P < 0.05$ and $P < 0.01$, respectively) compared with controls (mean: 1.17 ± 1.17, n = 6) (Fig. 5B). However, both PEG and PEG (device) groups showed a significant amount of tract discontinuities at the repair site.

Immunohistochemistry of Sciatic Nerves

Motor axons stained for choline acetyltransferase were counted from paraffin-embedded cross sections from animals that underwent electrophysiology and behavioral assessments at 1 week (n = 18), 4 weeks (n = 18), and 12 weeks (n = 18) postoperatively for control, PEG, and PEG (device) groups (Fig. 6). Axons outside the epineurium were eliminated for counting purposes. Counts were made from 10× photomicrographs of cross sections 5 mm proximal and 5 mm distal to the repair site by the presence of choline acetyltransferase stain. Axon counts in the proximal section of sciatic nerve did not differ significantly between any of the groups at any time point (1 week, 4 week, and 12 weeks). In the distal stump, PEG nerves demonstrated a significant increase in the number of axons compared with controls at 1 week and 4 weeks postoperatively ($P < 0.01$), but not at 12 weeks. The PEG (device) nerves had a significant increase in the number of motor axons distal to the repair site at 1 week, 4 weeks, and 12 weeks postoperatively compared with control nerves ($P < 0.001$, $P < 0.001$, and $P < 0.01$, respectively). Furthermore, PEG (device) animals displayed a statistically significant increase in distal motor axon counts at 4 weeks and 12 weeks postoperatively compared with PEG animals. Control, PEG, and PEG (device) animals all displayed a decrease in distal axons counts from 1 week to 4 weeks postoperatively (28%, 36%, and 8%, respectively). This decline was followed by an increase in the number of distal axons at 12 weeks postoperatively for all groups.

Representative photomicrographs imaged at 20×, show differences in motor axon morphology between each of the 3 groups at 1 week, 4 weeks, and 12 weeks postoperatively (Fig. 7). Control, PEG, and PEG (device) groups at 1 week all contain axons of increased axonal caliber and uneven staining. Control nerves at 4 weeks postoperatively (Fig. 7B) on average seems to be composed of axons of significantly smaller diameter that appear mostly around the inner edges of the epineurium. The PEG and PEG (devices) cross sections at 4 weeks (Fig. 7E, H) are composed of 2 populations of motor axons: large diameter and small diameter axons distributed evenly throughout the epineurium. At 12 weeks, postoperatively control nerves display a more uniform distribution of axons, however, as reflected in the axon counts (Fig. 6) PEG and PEG (device) nerves have a more dense distribution of axons within the epineurium.

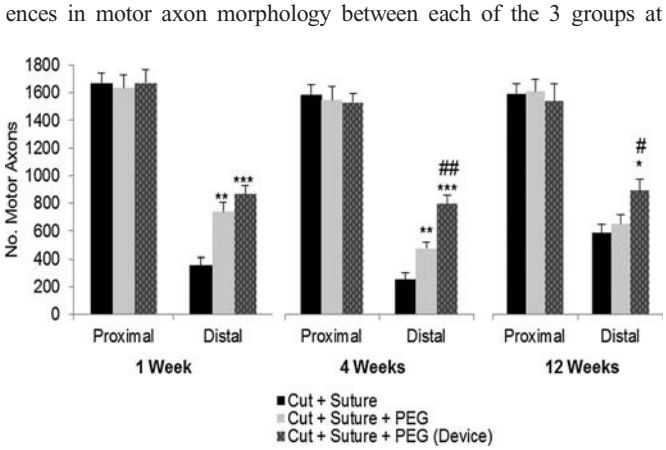

FIGURE 6. Motor axon counts (mean ± SE) from cross sections both proximal and distal to the repair site at 1 week, 4 weeks, and 12 weeks postoperatively. The PEG (device) significantly increased the number of distal axons compared with controls. Significance comparisons between control and both PEG groups are indicated by *, **, ***: $P < 0.05$, $P < 0.01$, and $P < 0.001$, respectively. Significance comparisons between PEG and PEG (device) groups are indicated by #, ##, ###.

Behavioral Evaluations of Sciatic Nerve Function

Behavioral assessments were evaluated from 3 days to 12 weeks postoperatively via the FF asymmetry (Fig. 8A, B) and SFI (Figs. 8C, D). Before surgery animals participated in habituation trials to acclimate as well as establish baseline control data. The FF and SFI scores ranging from −10 to +10 represent normal sciatic nerve function. To prevent possible bias, behavioral testers were blinded to the surgical protocols of each animal. In addition, all FF scores showed a statistically significant correlation ($r^2 = 0.56$, $P < 0.001$) with SFI scores graphed for each individual animal at all time points (Fig. 8E). Control animals demonstrated minimal behavioral recovery, with FF and SFI scores ranging from −94 to −72 and −101 to −84, respectively. The PEG animals demonstrated significantly improved FF scores at all but 1 time point (5 W; $P = 0.062$) compared with controls. The SFI scores showed a similar trend with PEG animals showing significantly improved scores at all time points ($P < 0.05$). The PEG (device) animals demonstrated statistically significant recovery of SFI and FF scores at all time points ($P < 0.01$) compared with controls.

Correlations Between Immunohistochemistry and Behavioral Assessments

Correlations between motor axon counts and SFI scores were evaluated at 1 week, 4 weeks, and 12 weeks (Fig. 9) postoperatively. A significant correlation was demonstrated at both 1 week ($r^2 = 0.56$, $P < 0.001$) and 4 weeks ($r^2 = 0.65$, $P < 0.001$). However, this positive correlation was lost at 12 weeks ($r^2 = 0.05$, $P > 0.05$). The loss of correlation at 12 weeks is due in large part to the increase in the number of motor axons in control animals with a lack of improvement in behavioral function, suggesting that the increased number of motor axons are not reestablishing functional connections with their respective muscle targets. However, a few outliers showing improved behavioral function with a lack of increased motor axon counts could point to axonal pruning. Further examination at the neuromuscular level is needed to confirm.

DISCUSSION

Because of the variety of fair to poor outcomes after traumatic injury to peripheral nerves in civilian and military populations, a substantial amount of research is being conducted to manipulate regeneration mechanisms in the hopes of improving clinical outcomes. Regardless of half a decade's worth of intense investigation, results after peripheral nerve injury are rather discouraging, with less than 50% of patients with proximal nerve injuries regaining "useful" function.[4] Currently, research strategies into peripheral nerve injury fall into 2 major categories: techniques to enhance axonal regeneration and techniques to decrease environmental inflammation. All of these experimental methods still rely on axons regenerating toward their end organ at a slow and lengthy rate of approximately 1 mm/d. A process that as previously mentioned often results in debilitating lifelong disability.

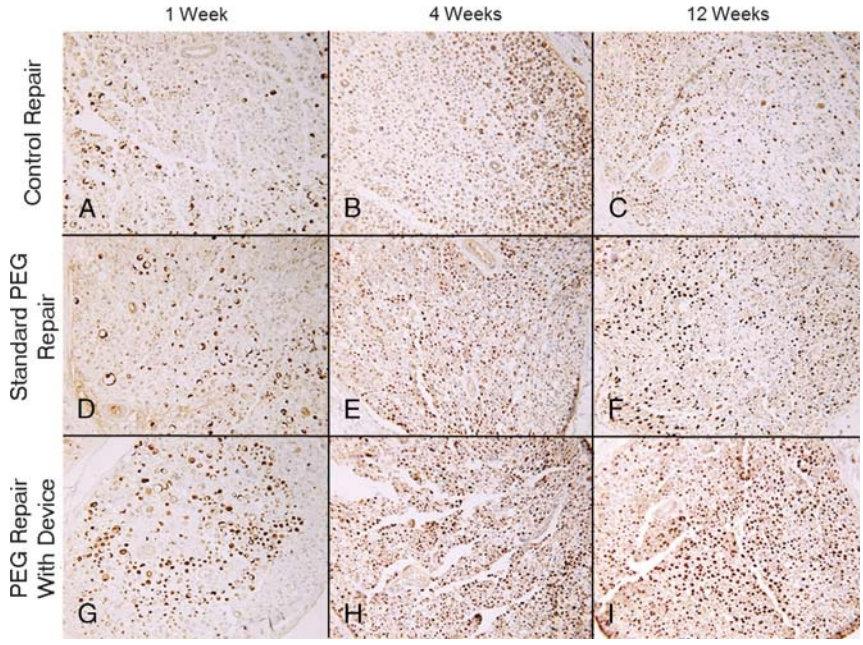

FIGURE 7. Representative photomicrographs of paraffin embedded cross section used for counts generated in Figure 4. Control (A–C), PEG (D–F), and PEG (device) (G–I) stained for choline acetyltransferase to label motor axons at 1 week (A, D, G), 4 weeks (B, E, H), and 12 weeks (C, F, I) postoperatively.

The aforementioned data suggest that PEG fusion may provide the ability to rapidly re-establish functional connections as well as rescue the distal stump from undergoing Wallerian degeneration. The loss of CAP (rodents) and electromyography (humans) signals are the earliest signs of axonal injury (ie, Wallerian degeneration).[28–30] These experiments further demonstrate that PEG directly restores electrophysiological functions immediately after surgical intervention. Furthermore, similar results were found using DTI as a diagnostic tool to verify the success of axonal fusion instantly after repair. The uptake of fluorescently labeled retrograde tracer in spinal motor neurons suggest that not only is axonal continuity maintained in the days after surgery, but that intra-axonal transport systems undergo rapid restructuring in successfully PEG-fused axons. A concern at the moment is that CAP amplitudes, number of fluorescently labeled cells, and DTI injury tracts in post PEG-fused animals are decreased compared with baseline controls. These findings suggest that PEG does not completely restore continuity to all axons within the epineurium. However, it does suggest restoration of a subset of axonal connections. The inability to have complete fusion of all axonal connections is most likely a result of surgical limitations to properly align axons within micrometers of one another as required for plasmalemmal fusion to occur. Therefore, we hypothesize that the percentage of axons displaying successful fusion depends heavily on the ability to achieve superior juxtapositioning before application of PEG.

Although immediate enhancement of nerve function is the goal of PEG fusion, it is vital that these connections maintain permanent viability. The histological findings from these studies suggest that motor axon counts within the epineurium are significantly increased within 1 week and maintained until 12 weeks postoperatively. The significant increase in the number of motor axons in PEG and PEG (device) animals at 1 week postoperatively compared with controls suggests that the process of Wallerian degeneration is prevented within a subset of successfully fused axons. The findings at 4 weeks and 12 weeks postoperatively suggest that axons initially preserved from Wallerian degeneration remain permanently viable. Although the data suggest that axonal fusion occurs at the cellular level, it certainly does not suggest that these axons are fusing with regard to individual axon specificity. Furthermore, it is possible that proximal portions of motor axons are fusing with distal portions of sensory axons. Currently, no evidence exists to suggest whether distal portions are reorganized by proximal portions, proximal portions are reorganized by distal portions, or whether higher central nervous system centers undergo rapid relearning.

Although morphological data is important to understanding the mechanism behind enhanced outcomes following PEG fusion, behavioral evaluations are often considered the most vital assessment of nerve function. Our data indicate that PEG significantly improves behavioral outcomes up to 25% by 3 days, 50% by 5 weeks, and is maintained until 12 weeks postoperatively according to the FF asymmetry and SFI. Correlations between behavioral assessments and motor axon counts suggest that further examination at the neuromuscular level is warranted. Our data indicate a significant correlation between the number of motor axons and behavioral outcomes at 1 and 4 weeks. However, this correlation is lost at 12 weeks postoperatively. This lack of correlation at 12 weeks is currently not understood and could be evidence of axonal pruning or nonfunctioning neuromuscular junctions. Previous studies in rodent models suggest an impaired capacity of regenerating axons to remake functional connections 8 weeks after injury. Therefore, the loss in correlation between axon counts and behavioral outcomes may be because of regenerating axonal outgrowths inability to reestablish functional connections with their respective muscle targets after 8 weeks postoperatively.

Surgical interventions to repair peripheral nerve injury have much better outcomes if completed earlier rather than later. Unfortunately, peripheral nerve injury is not often treated surgically within the ideal window for surgical intervention.[25,31] In large part, this is because of the fact that no diagnostic test exists to differentiate between different grades (specifically Sunderland types II and IV) of nerve injury.[3] Peripheral nerve injury does not have criterion standard diagnostic imaging studies. High-resolution ultrasound has shown the ability to accurately identify transected nerves, however, traumatic injuries have proven difficult for diagnosis using ultrasonography because of large hematomas, extensive skin lacerations, edema, and disruption of the

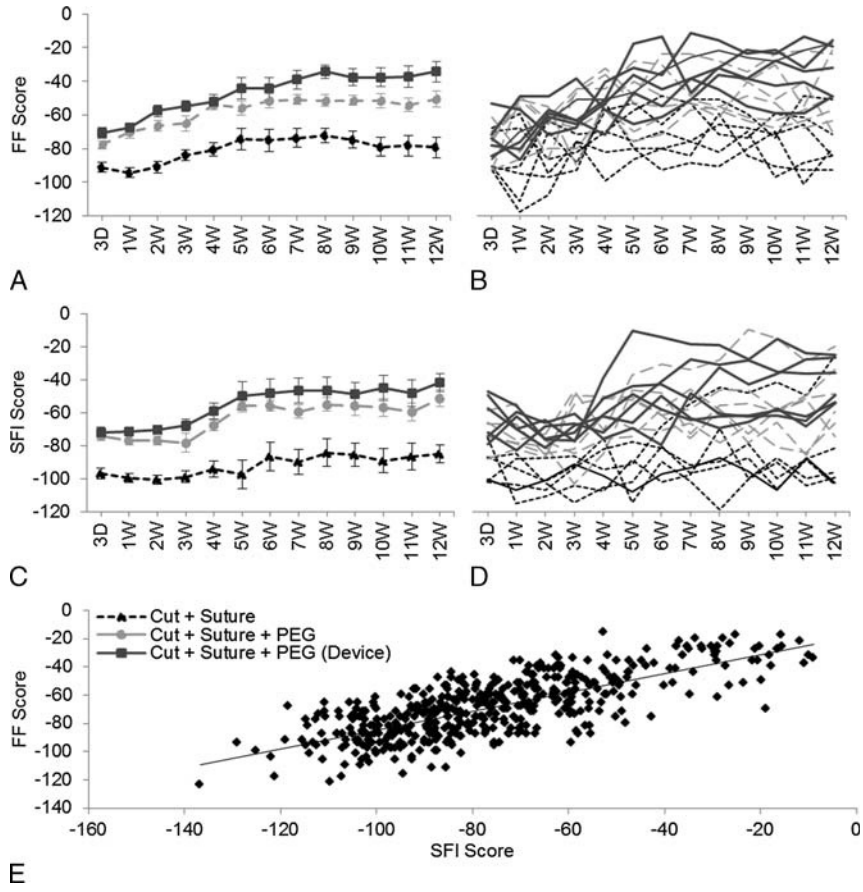

FIGURE 8. Behavioral assessments of sciatic nerve function according to the FF asymmetry test (A, B) and sciatic functional index (C, D). The FF and SFI scores (A, C: mean ± SE) were assessed from 3D to 12 weeks postoperatively for 3 groups: control (black dotted line), PEG (light-gray dotted line), and PEG (device) (dark gray solid line). Individual animals (B, D) for all 12 weeks animals were graphed according to the aforementioned group color scheme. E, Behavioral correlates indicate a highly significant ($P < 0.001$) positive correlation between SFI and FF scores.

normal anatomy. Furthermore, no studies have shown the ability of high-resolution ultrasonography to detect early nerve regeneration, which ultimately would indicate whether additional surgical intervention is required. DTI is an imaging modality that could revolutionize nerve injury evaluation. DTI yields quantitative metrics that report axonal integrity and demyelination. Here, we present findings that high-resolution DTI is not only capable of noninvasively detecting complete nerve transection but also capable of validating the success of PEG-fusion post-surgical intervention. The data suggests that DTI could have vast implication as a diagnostic tool in determining whether a nerve fusion was a success or failure. Although similar methods exist to assess morphological continuity (electrophysiology, histology, and fluorescent tracers), DTI is unique in that it has potential as in vivo method that is capable of assessing axonal continuity and viability over periods of time in the same animal. In addition, DTI is a technique that could be readily transitioned to the clinic to assess PEG fusion and peripheral nerve regeneration. A current limitation of PEG fusion is that no studies have determined the amount of time following injury that axons can be successfully fused and maintained. The use of DTI could rapidly expedite the process of physicians deciding whether further surgical intervention (ie, refusion) is necessary. A setback at the moment is the large degree of variation in DTI measurements that are influenced by confounding effects of edema and inflammation. In the future, the use of multicompartment diffusion-MRI models may help isolate these effects and deliver more consistent results among groups. In addition, nerves scanned for DTI in this study were excised and fixed. However, preliminary data not presented on amputated rat hind limbs have revealed success with only minor complications from surrounding tissue and edema.

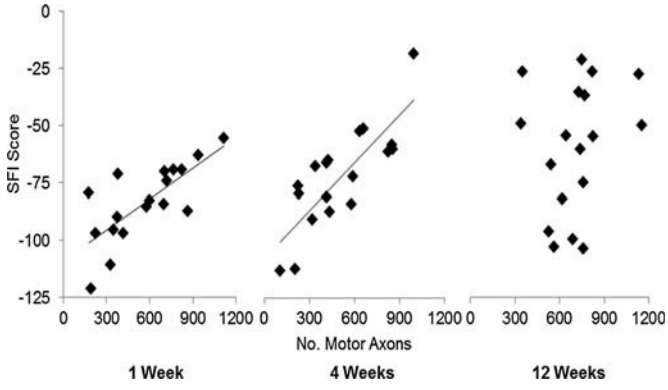

FIGURE 9. Correlation between motor axon counts (Fig. 6) and SFI score (Fig. 8) at 1 week (n = 18), 4 weeks (n = 18), and 12 weeks (n = 18) postoperatively. At 1 week and 4 weeks postoperatively, animals showed a significant correlation between distal axon counts and functional recovery. At 12 weeks postoperatively, no significant correlation between axon count and behavioral assessment was found.

The importance of a simplified PEG-fusion delivery device is evident from previous inconsistencies in functional, behavioral, and histological studies using PEG.[19,21–23] Our findings suggest that while PEG (device) animals were associated with a statistically significant increase in the number of distal motor axons at 4 and 12 weeks postoperatively, they were not associated with a significant improvement in CAP restoration, number of retrograde labeled cells, DTI tracts, or behavioral outcomes compared with PEG (no device) animals. Analysis of individual animals as seen in Figures 8B and 8D suggest that the higher level of significance seen in PEG (device) compared with PEG animals is due in large part to the increased consistency of successful fusions and not necessarily the level of recovery. These data suggest inconsistencies in the manual application of PEG and the need for further investigation into a simplified and more consistent method of PEG delivery.

The limited numbers of studies to date that evaluate the efficacy of PEG fusion have occurred in an acute setting, typically within an hour of injury. Clinically, it is more common to see nerve repairs occur after several hours, if not days, after nerve severance. Our current studies are focused on determining the time point at which successful PEG fusion repairs can occur and maintain long term viability after nerve severance. The ability to determine a timeframe in which successful PEG fusion may occur is vital to implementation of PEG fusion in a clinical setting in the future.

REFERENCES

1. Lundborg G. Richard P. Bunge memorial lecture. Nerve injury and repair–a challenge to the plastic brain. *J Peripher Nerv Syst*. 2003;8:209–226.
2. Kouyoumdjian JA. Peripheral nerve injuries: a retrospective survey of 456 cases. *Muscle Nerve*. 2006;34:785–788.
3. Grinsell D, Keating CP. Peripheral nerve reconstruction after injury: a review of clinical and experimental therapies. *Biomed Res Int*. 2014;2014:698256.
4. Lee SK, Wolfe SW. Peripheral nerve injury and repair. *J Am Acad Orthop Surg*. 2000;8:243–252.
5. Ma CH, Omura T, Cobos EJ, et al. Accelerating axonal growth promotes motor recovery after peripheral nerve injury in mice. *J Clin Invest*. 2011;121:4332–4347.
6. Scheib J, Hoke A. Advances in peripheral nerve regeneration. *Nat Rev Neurol*. 2013;9:668–676.
7. Giuffre JL, Kakar S, Bishop AT, et al. Current concepts of the treatment of adult brachial plexus injuries. *J Hand Surg Am*. 2010;35:678–688; quiz 688.
8. Saliba S, Saliba EN, Pugh KF, et al. Rehabilitation considerations of a brachial plexus injury with complete avulsion of c5 and c6 nerve roots in a college football player: a case study. *Sports health*. 2009;1:370–375.
9. Birch R, Booney G, Wynn-Parry CB. Clinical aspects of nerve injury. In: *Surgical Disorders of the Peripheral Nerve*. London: Churchill Livingstone; 1998:71–87.
10. Bittner GD, Schallert T, Peduzzi JD. Degeneration, trophic interactions, and repair of severed axons. *Neuroscientist*. 2000;6:88–109.
11. Hoy RR, Bittner GD, Kennedy D. Regeneration in crustacean motoneurons: evidence for axonal fusion. *Science*. 1967;156:251–252.
12. Kohler G, Milstein C. Continuous cultures of fused cells secreting antibody of predefined specificity. *Nature*. 1975;256:495–497.
13. Bittner GD, Ballinger ML, Raymond MA. Reconnection of severed nerve axons with polyethylene glycol. *Brain Res*. 1986;367:351–355.
14. Lore AB, Hubbell JA, Bobb DS Jr, et al. Rapid induction of functional and morphological continuity between severed ends of mammalian or earthworm myelinated axons. *J Neurosci*. 1999;19:2442–2454.
15. Krause TL, Bittner GD. Rapid morphological fusion of severed myelinated axons by polyethylene glycol. *Proc Natl Acad Sci U S A*. 1990;87:1471–1475.
16. Yogev D, Todorov AT, Qi P, et al. Laser-induced reconnection of severed axons. *Biochem Biophys Res Commun*. 1991;180:874–880.
17. Todorov AT, Yogev D, Qi P, et al. Electric-field-induced reconnection of severed axons. *Brain Res*. 1992;582:329–334.
18. Britt JM, Kane JR, Spaeth CS, et al. Polyethylene glycol rapidly restores axonal integrity and improves the rate of motor behavior recovery after sciatic nerve crush injury. *J Neurophysiol*. 2010;104:695–703.
19. Bittner GD, Keating CP, Kane JR, et al. Rapid, effective, and long-lasting behavioral recovery produced by microsutures, methylene blue, and polyethylene glycol after completely cutting rat sciatic nerves. *J Neurosci Res*. 2012;90:967–980.
20. Pannuzzo M, De Jong DH, Raudino A, et al. Simulation of polyethylene glycol and calcium-mediated membrane fusion. *J Chem Phys*. 2014;140:124905.
21. Sexton KW, Pollins AC, Cardwell NL, et al. Hydrophilic polymers enhance early functional outcomes after nerve autografting. *J Surg Res*. 2012;177:392–400.
22. Riley DC, Bittner GD, Mikesh M, et al. Polyethylene glycol-fused allografts produce rapid behavioral recovery after ablation of sciatic nerve segments. *J Neurosci Res*. 2015;93:572–583.
23. Rodriguez-Feo CL, Sexton KW, Boyer RB, et al. Blocking the P2X7 receptor improves outcomes after axonal fusion. *J Surg Res*. 2013;184:705–713.
24. Mueller MA, Zaydfudim V, Sexton KW, et al. Lack of emergency hand surgery: discrepancy between elective and emergency hand care. *Ann Plast Surg*. 2012;68:513–517.
25. Campbell WW. Evaluation and management of peripheral nerve injury. *Clin Neurophysiol*. 2008;119:1951–1965.
26. Sedy J, Urdzikova L, Jendelova P, et al. Methods for behavioral testing of spinal cord injured rats. *Neurosci Biobehav Rev*. 2008;32:550–580.
27. de Medinaceli L, Freed WJ, Wyatt RJ. An index of the functional condition of rat sciatic nerve based on measurements made from walking tracks. *Exp Neurol*. 1982;77:634–643.
28. Chaudhry V, Cornblath DR. Wallerian degeneration in human nerves: serial electrophysiological studies. *Muscle Nerve*. 1992;15:687–693.
29. Gilliatt RW, Hjorth RJ. Nerve conduction during Wallerian degeneration in the baloon. *J Neurol Neurosurg Psychiatry*. 1972;35:335–341.
30. Lunn ER, Brown MC, Perry VH. The pattern of axonal degeneration in the peripheral nervous system varies with different types of lesion. *Neuroscience*. 1990;35:157–165.
31. Flores AJ, Lavernia CJ, Owens PW. Anatomy and physiology of peripheral nerve injury and repair. *Am J Orthop (Belle Mead NJ)*. 2000;29:167–173.